Epitaxial Electrodeposition of Lead Sulfide on (100)-Oriented Single-Crystal Gold**

Alexey A. Vertegel, Mark G. Shumsky, and Jay A. Switzer*

Single-crystal films are important for device applications because the properties of the material of interest are not affected by the presence of grain boundaries. Epitaxial films are usually synthesized by vapor deposition onto a single crystal substrate, chosen to have a crystal structure and lattice parameter a as close as possible to that of the film. Typically, the lattice mismatch between a film and a substrate ($(a_{film} - a_{substrate})/a_{substrate}$) should not exceed 10–15%. Recently, we reported that epitaxial films of δ-Bi_2O_3 can be electrodeposited from an alkaline tartrate solution onto single-crystal Au,[1] although the lattice mismatch between δ-Bi_2O_3 and Au is 35.4%. The large mismatch was accommodated by forming coincidence lattices, in which the δ-Bi_2O_3 film was rotated in relation to the gold substrate. Herein, we extend this work to the electrodeposition of epitaxial films of lead sulfide (PbS) onto a single-crystal Au (100) substrate. The epitaxial films were deposited directly from solution precursors and required no subsequent thermal annealing to effect epitaxy. The crystal structures of Au and PbS are shown in Figure 1. Both structures are face centered cubic ($Fm3m$) with lattice parameters 0.4079 nm and 0.5933 nm, respectively. The lattice mismatch between the two materials is 45.5%.

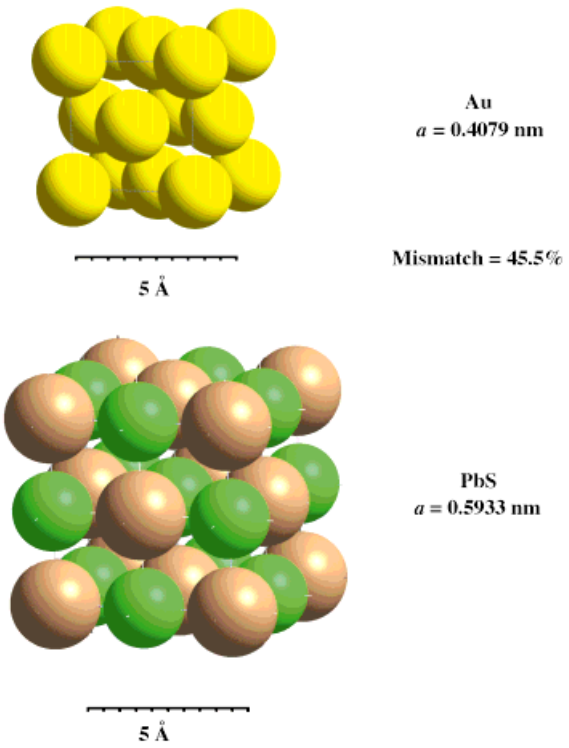

Figure 1. Crystal structures of Au and PbS. Both structures are face-centered cubic, space group $Fm3m$, with lattice parameters of 0.4079 and 0.5936 nm, respectively. The lattice mismatch between the two materials is 45.5%. Au atoms are yellow, Pb atoms are brown, and S atoms are green.

Several methods have been used to achieve epitaxial growth from solutions, including chemical bath deposition,[2] underpotential electrodeposition,[3] and electrochemical atomic layer epitaxy.[4] Epitaxial quantum dots of Cd(Se,Te) have been electrodeposited on evaporated Au(111) films.[5] Epitaxial CdS nanocrystals have been prepared on graphite by a hybrid electrochemical/chemical method.[6] However, little work has been done on the electrodeposition of epitaxial semiconductor films with thicknesses in the micrometer range. Lincot et al. reported the electrodeposition of epitaxial CdTe films onto InP(111) substrates.[7] Epitaxial films of PbO_2 have been deposited on TiO_2 and $SrTiO_3$ substrates by a photoelectrochemical method.[8] Single-crystal Bi films were deposited on Au-covered, single-crystal Si(100) by electrodeposition with subsequent annealing at 268 °C.[9]

Lead sulfide is a low band-gap (0.4 eV) semiconductor that is used extensively in IR photodetectors.[10] Polycrystalline films of PbS have been prepared by precipitation,[11] vacuum evaporation,[12] and chemical bath deposition.[13] Electrodeposition of PbS has been performed by anodic oxidation of S^{2-} on a Pb electrode,[14] by deposition from an acidic solution of $Pb(NO_3)_2$ and $Na_2S_2O_3$[15–16] and by co-reduction of Pb^{2+} and elemental sulfur in a suitable nonaqueous solvent.[17] However, the mobility of carriers in polycrystalline PbS films is two orders of magnitude less than that of the bulk material,[18] which results in a loss in sensitivity. Epitaxial PbS films should possess higher collection efficiency and better photoconductive properties.

The PbS films were electrodeposited on single-crystal Au(100) at 25 °C from an acidic (pH 4.0) solution of 0.1 M $[Pb(S_2O_3)_2]^{2-}$ in an excess of $S_2O_3^{2-}$. It should be noted that the authors of refs. [15–16] used lower concentrations of both components (ca. 10^{-3} M), probably to avoid precipitation of PbS_2O_3. However, the use of low concentrations imposes some limitations on the process conditions. In particular, PbS films were obtained only in the pH range 2.7–2.9.[16] In our preliminary experiments we did not see such an extreme pH effect. However, since colloidal sulfur may play an important role[15] the process should be performed at pH < 4.5 to achieve the following partial disproportionation of thiosulfate ions [Eq. (1)].

$$S_2O_3^{2-} + 2H^+ \rightarrow S_{colloidal} + SO_2 + H_2O \quad (1)$$

Figure 2 shows the Bragg–Brentano X-ray pattern for a PbS film on Au(100). Only the (200) and (400) peaks of PbS are observed, which indicates its strong out-of-plane orientation. Rocking curves performed on the (200) reflections of both Au and PbS gave full-width at half maximum (FWHM) values of 0.6 and 1.0°, respectively, indicating a high structural perfection of the film. In order to prove the in-plane

[*] Prof. J. A. Switzer, Dr. A. A. Vertegel, Dr. M. G. Shumsky
University of Missouri-Rolla
Department of Chemistry and
Graduate Center for Materials Research
Rolla, MO 65409-1170 (USA)
Fax: (+1) 573-341-2071
E-mail: jswitzer@umr.edu

[**] This work was supported by the National Science Foundation (CHE-9816484 and DMR-9704288) and the University of Missouri Research Board.

  1433-7851/99/3821-3169 $ 17.50+.50/0

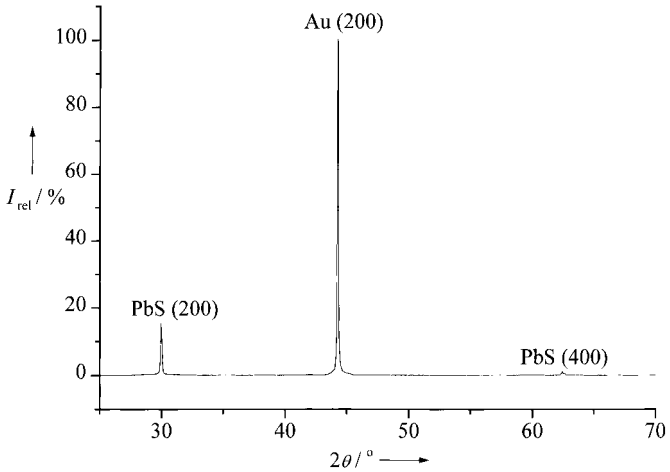

Figure 2. Bragg–Brentano X-ray diffraction pattern probing the out-of-plane orientation of a 1-μm thick PbS film electrodeposited onto single-crystal Au(100). Only the (*h*00) planes are observed in the X-ray pattern for both the film and substrate.

orientation and determine the epitaxial relationship between the film and substrate pole figures of the (111) reflections of PbS and Au were acquired. Figures 3A and B show the (111) pole figures for Au and PbS. In both cases, the expected fourfold symmetry is observed, with the peaks at a tilt angle $\chi \approx 55^\circ$. This angle corresponds well to the angle between the (111) and (200) planes (54.4°). No diffraction maxima are observed at other angles, which indicates the absence of any other epitaxial relations. The (111) reflections of PbS are observed at the azimuthal angles rotated 45° with respect to those of (111) reflections of Au, as shown in the azimuthal scan (Figure 3C). This means that although both the film and the substrate adopt the same (100) out-of-plane orientation, the PbS structure is rotated 45° with respect to the Au in the azimuthal plane. An interface model consistent with this rotation is Au(100)/$(\sqrt{2} \times \sqrt{2}\mathrm{R}45^\circ)$ – PbS(100), where R45° denotes the 45° rotation of the overlayer (Figure 4). In this case, the mismatch is only +2.9%. An SEM micrograph of the sample is presented in Figure 5. The film surface consists of square terraces characteristic of a (100) single crystal with a cubic structure. The square features are aligned with each other, and this is also consistent with the in-plane orientation of the film.

Studies of the detailed mechanism of the formation of epitaxial PbS films on Au(100) are currently in progress. Our preliminary results indicate that the primary electrochemical reaction most likely involves the reduction of Pb^{II} as shown in Equation (2).

$$[Pb(S_2O_3)_2]^{2-} + 2e^- \rightarrow Pb + 2S_2O_3^{2-} \quad (2)$$

The freshly deposited lead may then react with elemental sulfur adsorbed on the electrode. Demir and Shannon[19] showed that sulfur forms a stable $(\sqrt{2} \times \sqrt{2})\mathrm{R}45^\circ$ atomic layer on single-crystal Au(100) during underpotential deposition. Thus, formation of PbS may occur by the deposition of Pb atoms at the unfilled sites on the S/Au lattice, which results in the coincidence lattice that we observed experimentally.

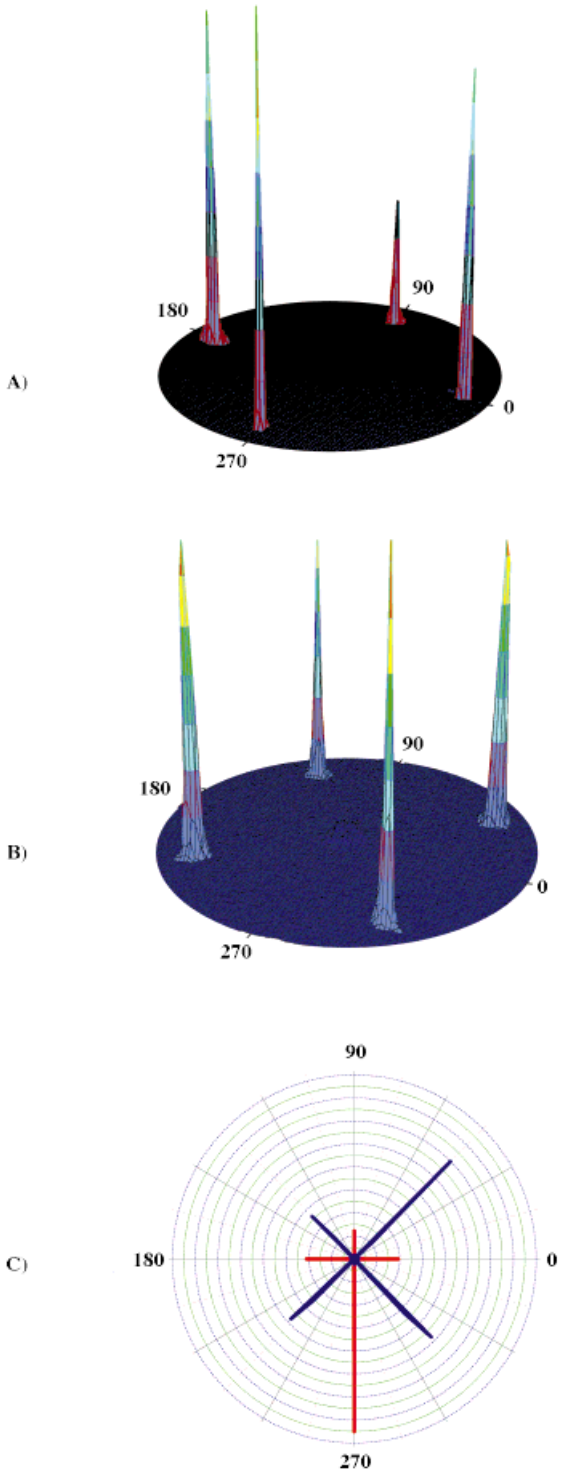

Figure 3. (111) pole figures for A) Au and B) PbS probing the in-plane orientation of the PbS film relative to the Au(100) substrate. The pole figures were obtained by setting 2θ equal to the angle of maximum diffracted intensity for the reflection of interest ($2\theta = 38.184^\circ$ and 25.963° for Au and PbS, respectively) and performing azimuthal scans at tilt angles (χ) from 0 to 70°. No other maxima are observed in either pole figure except for those occuring at $\chi \approx 55^\circ$. C) Azimuthal scans for the (111) reflection of Au (red) and PbS (blue). Each scan represents a cross section of the corresponding pole figure at the fixed tilt angle of 54.4°. This is the angle between the (111) and (200) planes in a cubic lattice. The (111) reflections for PbS are rotated 45° with respect to those of the substrate. The lobes of the azimuthal scan are not of equal intensity because of a slight misorientation of the Au single crystal. The average FWHM for the Au peaks is 1.2°, while the average FWHM for the PbS peaks is 1.8°.

  1433-7851/99/3821-3170 $ 17.50+.50/0

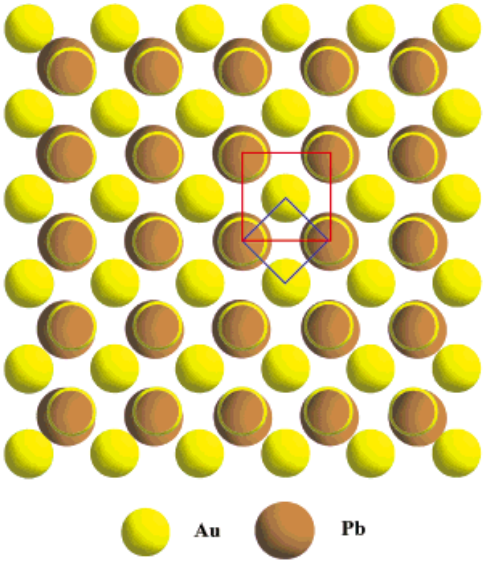

Figure 4. Schematic representation of the Au(100)/($\sqrt{2} \times \sqrt{2}$R45°) – PbS(100) coincidence lattice, which is consistent with the X-ray diffraction results. Sulfur atoms are not shown for clarity. The atoms of the adlattice are shown on top of the substrate atoms though they may actually occupy the hollow sites. The Au atoms placed beneath Pb atoms are shown as yellow rings. The red and blue squares indicate unit meshes of PbS and Au surface nets, respectively. The mismatch of the PbS coincidence lattice with the Au is +2.9%.

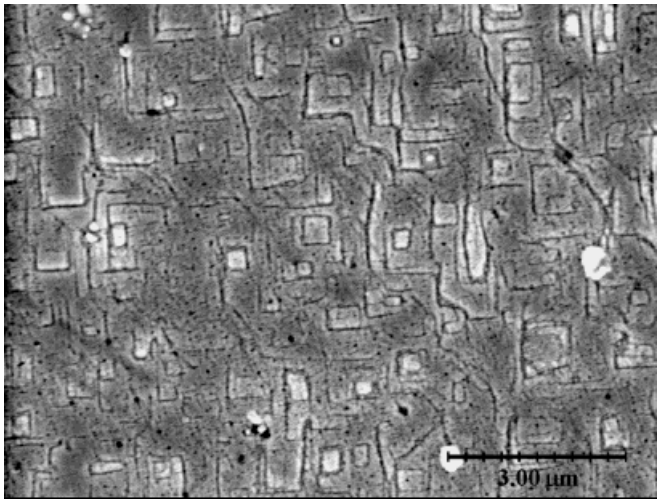

Figure 5. SEM micrograph of the PbS film. Note the square terraces are aligned with each other, which are characteristic of (100) surfaces of cubic single crystals.

Experimental Section

The deposition solution was prepared by adding 1M aqueous $Na_2S_2O_3$ to 0.25M $Pb(NO_3)_2$ with vigorous stirring. A white precipitate of PbS_2O_3 is first formed, which then dissolves in the excess of thiosulfate to form $[Pb(S_2O_3)_2]^{2-}$. The concentrations of the components in the final solution were 0.1M Pb^{2+} and 0.6M $S_2O_3^{2-}$. This ratio ensures full dissolution of PbS_2O_3. The final pH of the solution was adjusted to pH 4.0 with 0.5M HNO_3. HPLC-grade water (Aldrich) was used to prepare the solutions. All other chemicals were reagent grade (Aldrich).

The working electrode consisted of an electropolished Au(100) single crystal (Monocrystals Company), with a diameter of 10 mm and a thickness of 1 mm. A gold wire was fitted around the edge of the crystal to serve as the electrical contact during deposition. The film was deposited only on one side of the crystal by using the meniscus method. The counter electrode consisted of a chromel alloy wire. A constant cathodic current density of 0.125 mA cm^{-2} was applied to the working electrode with an EG&G Princeton Applied Research Model 273A potentiostat/galvanostat for 5000 s to yield a nominal PbS film of thickness 1 µm.

X-ray diffraction experiments were performed ex-situ in air with a Scintag 2000 diffractometer using $Cu_{K\alpha}$ radiation. The 2θ scan was performed with a step size of 0.03° and a data acquisition time of 1 s per point. Azimuthal scans were obtained by the use of a texture goniometer accessory that had been fashioned in-house for the Scintag 2000 diffractometer. The azimuthal steps were 1° with a data acquisition time of 1 s per point. SEM micrographs were carried out on a Hitachi model S4700 cold-field emission scanning electron microscope.

Received: June 7, 1999 [Z13527IE]
German version: *Angew. Chem.* **1999**, *111*, 3363 – 3366

Keywords: electrochemistry · epitaxy · lead sulfide · semiconductors · surface chemistry

[1] J. A. Switzer, M. G. Shumsky, E. W. Bohannan, *Science* **1999**, *284*, 293.
[2] a) J. L. Davis, M. K. Norr, *J. Appl. Phys.* **1966**, *37*, 1670; b) H. Rahnamai, H. J. Gray, J. N. Zemel, *Thin Solid Films* **1980**, *69*, 347.
[3] A. Aramata, *Mod. Aspects Electrochem.* **1997**, *31*, 181.
[4] L. Colletti, B. H. Flowers, Jr., J. L. Stickney, *J. Electrochem. Soc.* **1998**, *145*, 1442.
[5] Y. Golan, L. Huchison, I. Rubinstein, G. Hodes, *Adv. Mater.* **1996**, *8*, 631.
[6] S. Gorer, J. A. Ganske, J. C. Hemminger, R. M. Penner, *J. Am. Chem. Soc.* **1998**, *120*, 9584.
[7] D. Lincot, B. Kampmann, B. Mokili, J. Vedel, R. Cortes, M. Froment, *Appl. Phys. Lett.* **1995**, *67*, 2355.
[8] Y. Matsumoto, M. Fujisue, T. Sasaki, J. Hombo, M. Nagata, *Appl. Phys. Lett.* **1994**, *369*, 251.
[9] F. Y. Yang, K. Liu, K. Hong, D. H. Reich, P. C. Searson, C. L. Chien, *Science* **1999**, *284*, 1335.
[10] V. Subramanian, K. R. Murali, N. Rangarajan, A. S. Lakshmanan, *Proc. SPIE Int. Soc. Opt. Eng.* **1994**, *2274*, 219.
[11] H. Hirata, K. Date, *Anal. Chem. Acta* **1972**, *60*, 405.
[12] A. K. Mady, A. Girgis, A. H. Mady, R. Moustaf, *Phys. Status Solidi A* **1987**, *100*, 107.
[13] K. M. Gadave, S. A. Jodgudri, C. D. Lokhande, *Thin Solid Films* **1994**, *245*, 7.
[14] B. Sharifker, Z. Ferreira, J. Mozota, *Electrochim. Acta* **1985**, *30*, 677.
[15] M. Takahashi, Y. Ohshima, K. Nagata, S. Furuta, *J. Electroanal. Chem.* **1993**, *359*, 281.
[16] M. Sharon, K. S. Ramaiah, M. Kumar, M. Neumann-Spallart, C. Levy-Clement, *J. Electroanal. Chem.* **1997**, *436*, 49.
[17] A. S. Baranski, W. R. Fawcett, *J. Electrochem. Soc.* **1980**, *127*, 766.
[18] F. L. Lummis, R. L. Petritz, *Phys. Rev.* **1957**, *105*, 502.
[19] U. Demir, C. Shannon, *Langmuir* **1996**, *12*, 594.

  1433-7851/99/3821-3171 $ 17.50+.50/0